Materials Science & Engineering A 763 (2019) 138163

Contents lists available at ScienceDirect

Materials Science & Engineering A

journal homepage: www.elsevier.com/locate/msea

Strengthening of Mg-based long-period stacking ordered (LPSO) phase with deformation kink bands

Koji Hagihara[a,*], Michiaki Yamasaki[b], Yoshihito Kawamura[b], Takayoshi Nakano[c]

[a] Department of Adaptive Machine Systems, Graduate School of Engineering, Osaka University, 2-1 Yamadaoka, Suita, Osaka, 565-0871, Japan
[b] Magnesium Research Center & Department of Materials Science, Kumamoto University, 2-39-1 Kurokami, Chuo-ku, Kumamoto, 860-8555, Japan
[c] Division of Materials and Manufacturing Science, Graduate School of Engineering, Osaka University, 2-1 Yamadaoka, Suita, Osaka, 565-0871, Japan

ARTICLE INFO

Keywords:
Deformation kink band
Basal slip
LPSO-Phase
Microstructure
Dislocation

ABSTRACT

The mechanical properties of the Mg-based LPSO-phase are expected to be strongly affected by the microstructure due to its anisotropic crystal structure. However, the fine details have not been sufficiently understood yet. This study first clarified the detailed microstructural factors that govern the strength of the LPSO-phase by examining alloys with microstructures that were significantly varied via directional solidification and extrusion processes. Refining the microstructure is significantly effective for strengthening LPSO-phase alloys. The yield stress of LPSO-phase alloys with random texture was previously reported to be increased by reducing the "length" of plate-like LPSO-phase grains. In addition, it was found in this study that the formation stress in the deformation kink band, which is a unique deformation mode in an LPSO-phase alloy, can be increased by decreasing the "thickness" of the grains. Furthermore, the study used directionally solidified crystals provided direct evidence that the introduction of the deformation kink band effectively increases the yield stress and work-hardening rate of alloys by hindering the motion of basal dislocations. This "kink-band strengthening" was found to have considerable temperature dependence. The strengthening is significant at or below 200 °C, but the effect gradually decreases above 300 °C and is accompanied by the operation of non-basal slip. The results quantitatively clarified that kink-band strengthening is one predominant reason why the LPSO-phase extruded alloy exhibits an unusually high yield stress at any loading orientation.

1. Introduction

The development of noble lightweight structural materials is desired for improving fuel efficiency of transportation equipment and vehicles [1], with the goal of overcoming global warming. To achieve this, the long-period stacking ordered (LPSO) phase has recently been the focus of much attention as an attractive strengthening phase for Mg alloys [2–16], especially in an Mg–Zn–Y ternary alloy system. The LPSO-phase has (0001) close-packed planes in common with the Mg phase with a hexagonal close-packed (hcp) structure, but its stacking sequence is largely lengthened along the *c* axis [17]. In order to clarify the strengthening mechanism of Mg/LPSO two-phase alloys, the mechanical properties and plastic deformation behavior of the LPSO-phase itself must be understood first. We examined this by using a textured LPSO-phase predominantly containing alloys prepared by a directional solidification (DS) process [18–20] and an extrusion process [21–23]. It was found that two deformation modes of the (0001) basal slip and the formation of the deformation kink band predominantly govern plastic deformation of the LPSO-phase. The deformation kink is a characteristic deformation band, which is believed to be formed by the avalanche generation of basal dislocation pairs in the restricted region, detailed features of which were discussed in a previous paper [18]. Operation of the other deformation modes is strongly hindered at low temperatures near ambient owing to the complicated atomic arrangement in the LPSO-phase.

Due to the limitation of the operative deformation mode, the plastic behavior of the LPSO-phase exhibits strong anisotropy, thus the mechanical properties are expected to largely vary with microstructure. Indeed, we found that the yield stress of the LPSO-phase extruded alloy with fine microstructure exhibited an extremely high value of around 460–480 MPa [21,23], which is almost triple that of a DS alloy. Nevertheless, both alloys exhibit similar basal fiber texture, in which the basal planes in the LPSO-phase grains were aligned parallel to the growth or extruded direction [18,21].

LPSO-phase grains in the alloys exhibited a peculiar plate-like morphology, with a wide and flat surface parallel to the (0001) plane

* Corresponding author.
E-mail address: hagihara@ams.eng.osaka-u.ac.jp (K. Hagihara).

https://doi.org/10.1016/j.msea.2019.138163
Received 2 April 2019; Received in revised form 13 June 2019; Accepted 14 July 2019
Available online 16 July 2019

[18]. During deformation of the alloy, where basal slip governs the plastic behavior, we previously elucidated that the yield stress (σ_y) could be estimated from the so-called Hall-Petch relation $\sigma_y = \sigma_0 + kd^{-1/2}$, when the length of the long-axis of the plate-like LPSO-phase grains is taken as the grain size d [21,22]. This occurs because the mean-free path of the basal dislocation is directly proportional to the average length of the long-axis of the grain size due to the peculiar plate-like shape of the LPSO-phase grains, whose flat surface is parallel to (0001) basal slip plane. On the other hand, the microstructural factor that governs the yield stress of the alloy, where generation of a deformation kink carries plastic deformation, has not yet been clarified.

In addition, the introduced deformation kink band itself is also considered to affect the mechanical properties of the alloy during further deformation. In the extruded alloy, many deformation kink bands are introduced during extrusion to accommodate stress concentration. The introduced kink bands are supposed to impede motion of basal dislocations [5,6,23], but this effect has not yet been quantitatively estimated. The deformation kink band is known to be formed in many materials that show strong plastic anisotropy, e.g., in metals [24], some minerals, organic crystals, rubber laminates, oriented polymer fibers, and woods [25]. In those materials, the deformation kink band acts as an important deformation mode to accommodate stress concentration. Therefore, clarification of the general nature of plastic deformation governed by the deformation kink is very important to obtain a comprehensive understanding of their deformation behavior, including Mg-based LPSO-phase alloys.

Based on this background, the controlling factor for plastic deformation of the LPSO-phase carried by the deformation kink band and the influence of the introduced deformation kink bands on further deformation were examined by using various DS and extruded alloys with greatly different microstructures. The obtained results were used to determine why an LPSO-phase extruded alloy exhibits an extremely high yield stress.

2. Experimental procedure

Mother $Mg_{88}Zn_5Y_7$ (at.%) ingots were prepared by induction melting in a carbon crucible. The DS process was conducted using the Bridgman technique in an Ar-gas atmosphere. The details of the preparation method were reported in a previous paper [18]. In this study, four DS crystals were grown at different crystal growth rates of 2.5, 5.0, 15.0, and 20.0 mm/h in order to modify the grain size of the alloys. Extruded LPSO-phase alloys were also prepared to obtain textured alloys with a much finer microstructure. This extrusion was conducted at 450 °C at an extrusion rate of 10:1 (indicated as R10 hereafter), using mother alloys with a composition of $Mg_{89}Zn_4Y_7$. In this study, two mother alloys with different microstructures were prepared for extrusion. One was prepared by casting into an iron mold with ~9.6 K/s cooling rate, as previously reported [21]. The other mother alloy was furnace cooled after melting, with the cooling rate controlled at ~0.036 K/s; see Ref. [6] for details on the estimation of the cooling rate. Extruded alloys with different LPSO-phase grain sizes were fabricated from these two mother alloys. The microstructures of these alloys were examined using an optical microscope (OM). The obtained DS and extruded alloys were dominantly composed of LPSO-phase grains, although a small amount of the $Mg_3Zn_3Y_2$ phase (W-phase) coexisted in the DS alloys and ~14 vol% of the Mg-phase coexisted in the extruded alloys, respectively. The textures of the alloys were examined using a pole figure analysis performed with an X-ray diffractometer (Bruker AXS, D8-DISCOVER with GADDS, and Philips, X'Pert PRO MPD). It was confirmed that both the DS and extruded alloys contained strong basal fiber textures, in which the basal planes in the LPSO-phase grains were aligned parallel to the growth or extrusion direction. The results on the textures are provided in previous papers [18,21].

The mechanical properties of the alloys were examined using compression tests. Rectangular specimens (approximately $2 \times 2 \times 5\,mm^3$) were cut using electrodischarge machining from the DS alloys or extruded alloys. Two loading directions were selected for testing. The first was parallel to the growth or extrusion direction, and the second was inclined at 45° to the former; hereafter, these are called the 0° and 45° orientations, respectively. At 45° orientation, the basal slip carries plastic strain. Meanwhile, the formation of a deformation kink band predominantly carries the strain at 0° orientation since the Schmid factor for basal slip is negligible due to the basal fiber texture [18,21]. Compression tests were performed on an Instron testing machine with $1.67 \times 10^{-4}\ s^{-1}$ nominal strain rate at ambient temperature.

In addition to those simple compression tests, "double compression tests" were conducted for the DS crystals grown at 5 mm/h in order to elucidate the influence of introducing the deformation kink bands on the yield stress and work-hardening behavior of the LPSO-phase alloy. First, a rectangular specimen (approximately $2 \times 5 \times 5\,mm^3$) with 0° loading axis was prepared from the DS crystal. This rectangular specimen was compressed up to 5% plastic strain at ambient temperature in order to introduce the deformation kink bands; this is called the "first deformation" hereafter. Then, a second compressive specimen with 45° loading axis was cut out from the deformed specimen, and the specimen was again compressed; this is called the "second deformation". The second set of compression tests at 45° loading were conducted at temperatures between room temperature and 400 °C. These tests were used to examine the influence of the introduced deformation kink bands on basal dislocation motion in the LPSO-phase, along with their temperature dependence. Deformation markings placed on the specimen surfaces were analyzed using the OM with Nomarski interference contrast.

3. Results

3.1. Influence of grain thickness on formation stress of deformation kink band in LPSO-phase alloys

We previously found that the operation of basal slip governs the plastic deformation behavior during deformation of an alloy with random texture [21]. In this case, the yield stress can be estimated using the Hall-Petch relation by assuming that the "length" of the plate-like shape of the LPSO-phase grain is the grain size [21,22]. On the other hand, when the stress is loaded along the 0° orientation axis in an alloy with basal fiber texture, i.e., the loading axis is parallel to the basal plane, basal slip is strongly hindered because its Schmid factor is negligible. Instead, the formation of the deformation kink band dominantly carries the plastic strain. In this situation, the mechanism governing the mechanical properties is not fully understood. According to a report by Barsoum et al. [26–28], there is a possibility that the "thickness" of the plate-like LPSO-phase grains controls the initiation stress of the deformation kink band. They investigated the plastic deformation behavior of a ceramic Ti_3SiC_2 alloy, along with other $M_{n+1}AX_n$-type phase alloys (so-called MAX-phases). They discussed the formation stress of the deformation kink band in these alloys, based on the theory first proposed by Frank and Stroh [29]. They suggested that the remote shear stress τ, which is required to render a kink band nucleus unstable and allow it to grow, is given as follows:

$$\tau > \sqrt{\frac{4G^2 b\gamma_C}{2\alpha\pi^2}\ln\left(\frac{b}{r\gamma_C}\right)} \quad (1)$$

where G is the shear modulus; b is the Burgers vector; γ_c is the critical kink angle (~0.05–~5° for most solids), r is a value related to the core energy of the dislocation, and 2α is the length of a kink band with elliptical shape [26–28]. This equation can only be used to estimate the remote shear stress for growth of an incipient deformation kink. Hence, the absolute value of the yield stress of the alloy cannot be directly

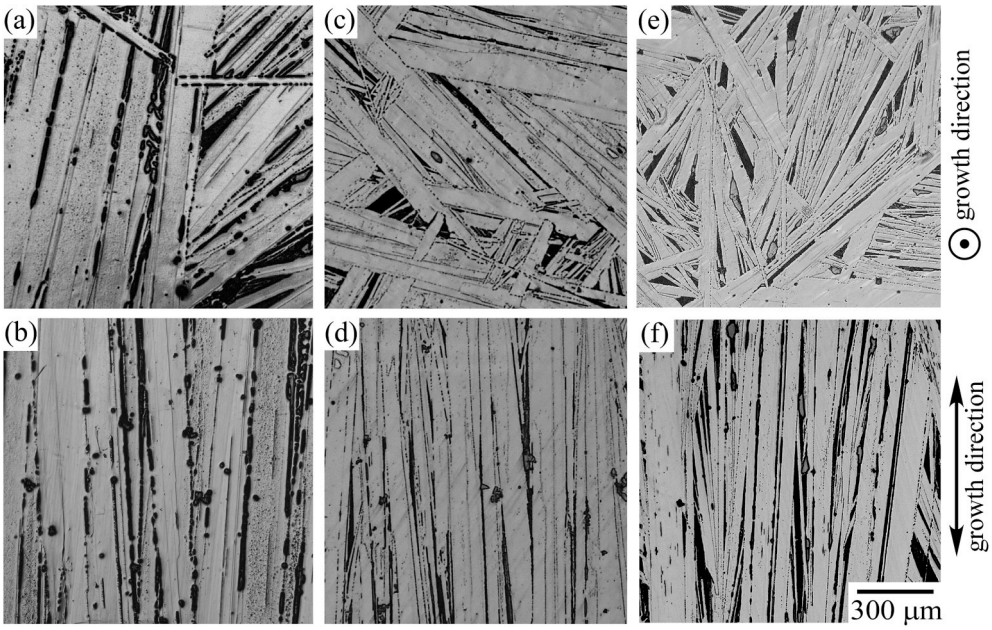

Fig. 1. OM images showing the microstructures of the DS crystals grown at (a, b) 2.5 mm/h, (c, d) 5 mm/h, and (e, f) 15 mm/h. Images were gathered from the (a, c, e) transverse sections and (b, d, f) longitudinal sections along the growth direction.

evaluated from this equation. However, it was suggested that the maximum length of the kink band (2α), from a geometric perspective, would be constrained by the grain thickness along the [0001] c-axis [26]. Therefore, this equation implies that refining the microstructure increases the formation stress of a deformation kink band in proportion to $(2\alpha)^{-1/2}$, which must induce an increase in the yield stress. As described in the introduction, the LPSO-phase grains show peculiar plate-like shapes with a broad interface which is parallel to the (0001) basal plane [18]. Therefore, there is a possibility that the mechanical properties of the LPSO-phase alloy in which the formation of the deformation kink band carries the strain may vary depending on the average grain thickness *t*. In order to confirm this experimentally, we examined variations in the yield stress of DS alloys as a function of grain thickness during compression tests at 0° orientation. Plastic deformation in the extruded alloys with much finer microstructures and similar (0001) basal fiber textures were also examined.

The grain thickness in the DS alloy was controlled by changing the growth rate in the Bridgman process. Fig. 1 shows the microstructures of the DS crystals grown at 2.5, 5, and 15 mm/h observed from the longitudinal and transverse sections with respect to the growth direction. One can clearly see that the (0001) plate-like grain interface grew nearly parallel to the growth direction. Therefore, examining the microstructure of a transverse section allows the average thickness of the grains to be measured. By increasing the growth rate from 5 mm/h to 15 mm/h, the average thickness of the LPSO-phase grain could be narrowed from ~101 μm to ~59 μm while still maintaining the aligned plate-like microstructure along the growth direction, as shown in Fig. 1(d) and (f). However, further increase in the crystal growth rate to 20 mm/h destroyed the aligned microstructure [30]. Hence, the formation stress of the deformation kink could not be evaluated using the crystal grown at 20 mm/h. On the other hand, when the growth rate of the DS crystal was decreased to 2.5 mm/h, the grain had a thickness of ~118 μm, as shown in Fig. 1(a) and (b).

Extrusion is a useful method for fabricating an alloy with similar basal fiber texture but much finer microstructure. During extrusion, two mother ingots were prepared in order to control the grain size. One ingot was fabricated by rapid casting into an iron mold, while the other ingot was fabricated by furnace cooling. Fig. 2 shows the microstructures of these two extruded alloys observed in longitudinal sections along the extrusion direction. As seen in the figures, the grain size of the LPSO-phase could be greatly varied using the two mother ingots. The average grain thickness was found to be ~10 μm for the cast alloy but as large as ~27 μm for the furnace cooled alloy; these values were determined by examining the microstructures on the transverse section. The plate-like LPSO-phase grains were well aligned after extrusion in both alloys. The plate-like interface of the LPSO-phase grain is known to be parallel to the (0001) basal plane [18]. Therefore, the microstructure shown in Fig. 2 obviously demonstrates that the alloys had a "basal fiber texture," in which the basal plane was parallel to the extrusion direction. In other words, the extruded alloys had texture similar to that in the DS alloys, as was previously confirmed from X-ray diffraction analysis results [21]. However, the interfaces of the LPSO-phase grains in the extruded alloys were not as flat as those in the DS alloys and instead exhibited sharp or round bends. This occurred due to the introduced deformation kink bands during extrusion for accommodating stress concentration [21,23].

Fig. 3 shows the deformation microstructures in the five DS and extruded specimens after deformation at 0° orientation and at room temperature. Deformation kink bands were abundantly formed and were the main carriers of plastic strain in all specimens. Non-basal slip, whose slip traces are not parallel to the plate-like grain interfaces, was found around the deformation kinks only in the extruded specimens due to their very high yield stresses, as indicated by blue arrows in Fig. 3(d and e). However, other large differences in the LPSO-phase grain deformation mechanism were not observed.

Fig. 4 shows the corresponding room temperature yield stresses of the DS and extruded alloys at 0° orientation as a function of the inverse of the square root of the average grain thickness ($t^{-1/2}$). The yield stresses of the DS crystals showed large scatter because the small disturbance to textures in the specimens significantly affected the yield stress. The average yield stress slightly increased as the thickness of the LPSO-phase grains decreased, as was briefly reported in the previous study [30]. However, this tendency is rather weak in the DS crystals and it cannot be strongly confirmed due to scatter in the data. This weak grain thickness dependence of yield stress in the DS crystal implies that the constrained effect affecting the size of grown kink-band nucleus by grain boundary is weak in such large grains.

On the other hand, this increasing tendency of yield stress was

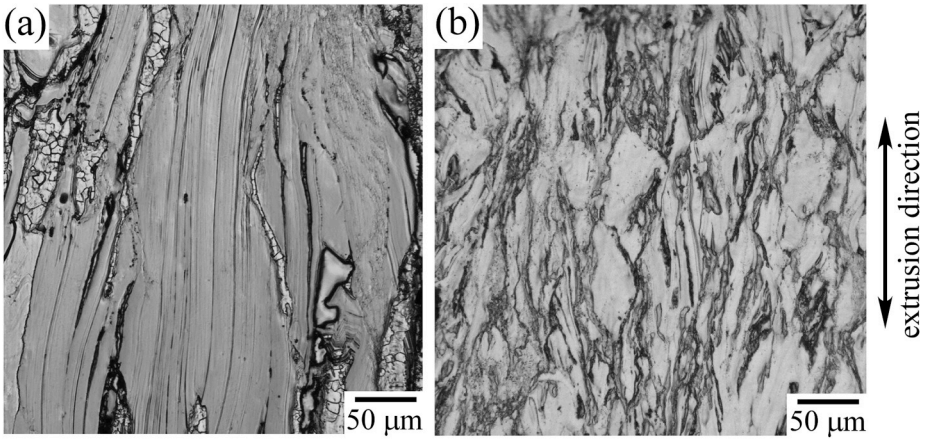

Fig. 2. Variation in the microstructures of extruded alloys as a function of solidification rate of the mother ingot used for extrusion. The microstructures were observed from the longitudinal sections along the extrusion direction. (a) Extruded alloy fabricated from the mother alloy that was furnace cooled at ~0.036 K/s. (b) Extruded alloy fabricated from the cast mother alloy that was cooled at ~9.6 K/s.

drastically enhanced in the extruded specimens with finer microstructure compared to that in DS crystals. From the present data, one cannot concluded with confidence whether or not the yield stress is proportional to the inverse of the square root of the grain thickness ($t^{-1/2}$) due to the limited amount of data. However, at least the results obviously demonstrate that the refined microstructure is very effective for strengthening an LPSO-phase alloy, not only by suppressing basal slip [19], but also by suppressing easy formation of deformation kink bands. This is due to the increased formation stress of the deformation kink via the reduced grain thickness, especially in the alloys with fine microstructures where the thickness of the LPSO-phase grain is less than ~50 μm.

3.2. Influence of deformation kink bands as obstacles to basal slip

As described in the previous section, deformation kink bands are frequently introduced during deformation in a stress field where the motion of basal dislocations is prohibited, and carry compressive strain. According to the model proposed by Hess and Barret [24], the interface of the deformation kink band is composed of an array of basal dislocations with edge character. The atomistic structure of the interface of

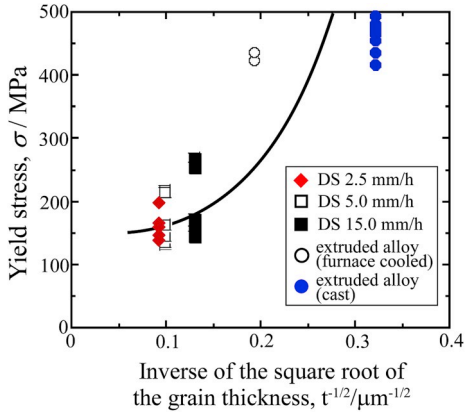

Fig. 4. Yield stresses of DS and extruded alloys deformed at 0° orientation and at room temperature as a function of the inverse square root of the average grain thickness ($t^{-1/2}$).

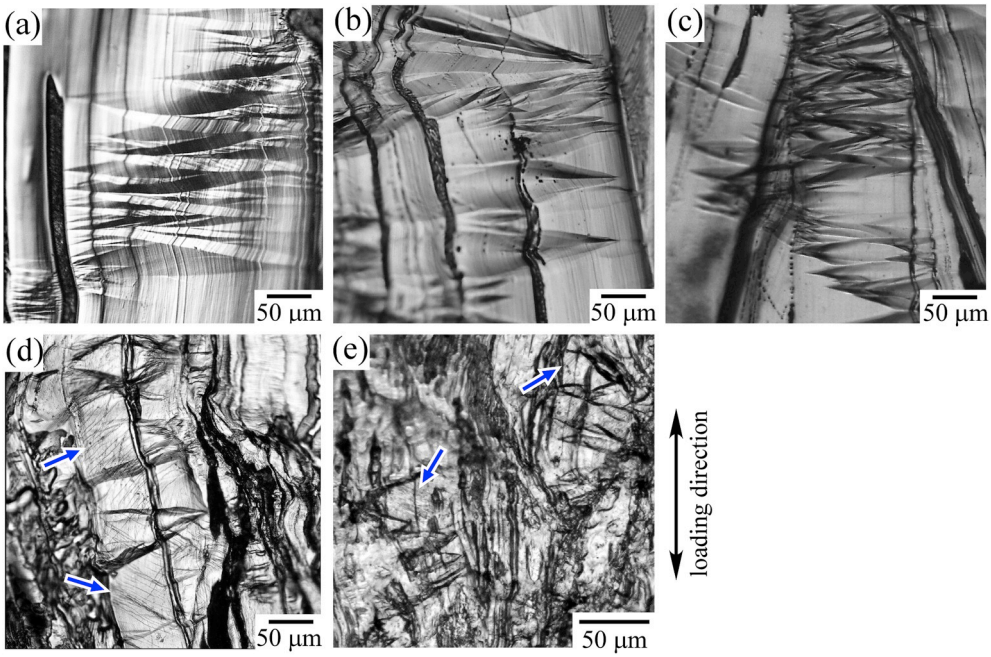

Fig. 3. Microstructures in DS and extruded specimens deformed at 0° orientation and at room temperature. DS specimens grown at (a) 2.5 mm/s, (b) 5.0 mm/s, and (c) 15.0 mm/s. (d) Extruded alloy fabricated from the furnace-cooled mother alloy and (e) extruded alloy fabricated from the cast mother alloy.

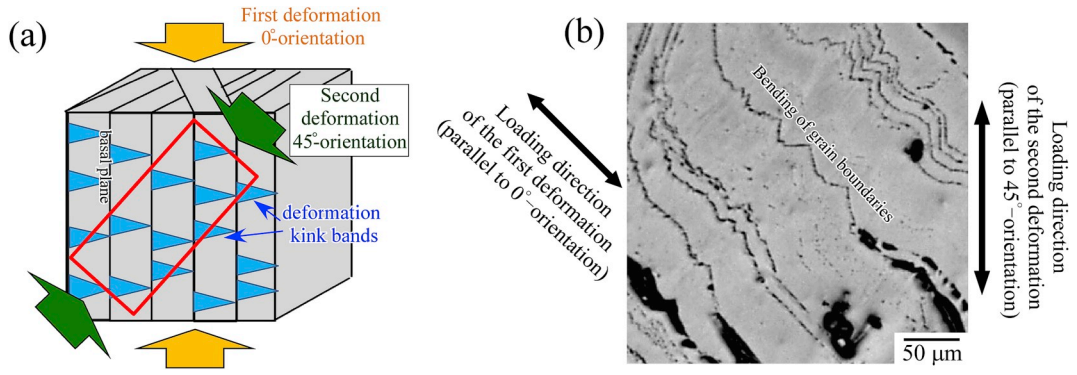

Fig. 5. (a) Schematic detailing the double compression test. (b) OM image showing the surface of specimen deformed at 0° orientation up to 5% plastic strain at room temperature. The sample was then mechanically and chemically polished, which corresponds to the specimen surface before the second deformation.

a deformation kink band in the LPSO-phase has been examined by several researchers [31–33], and similar features were reported in the deformation kink bands with low rotation angles [32,33]. In addition, regarding the deformation kink band boundary in the LPSO phase, segregation of Zn and Y atoms was reported recently [31,32]. It is thus expected that the deformation kink boundary would act as an obstacle to subsequent motion of basal dislocations, similar to the grain boundary. This must affect the yield stress and work-hardening behavior of the alloy. Double compression tests were conducted in this study in order to evaluate this effect quantitatively. The method is schematically shown in Fig. 5(a). First, large rectangular DS crystal specimens with 0° loading axis were prepared and compressed up to 5% plastic strain at room temperature (first deformation). Small specimens with the 45° loading axis were cut out from these deformed crystals and were subsequently deformed (second deformation). The influence of deformation kink as an obstacle to the basal slip was examined by comparing the plastic behavior of the double-deformed specimens with that of the un-predeformed specimens (called “virgin specimens” hereafter).

Fig. 5(b) shows the microstructure of a specimen that was first deformed at 0° orientation and whose surface was then mechanically and chemically polished. A large number of deformation kink bands were introduced by the first deformation at 0° orientation. Hence, the interfaces of the plate-like grains were significantly bent in a zigzag manner. It should be noted here that few cracks were introduced at the interface, despite the significant grain bending as a result of the deformation kinking. The deformation kink bands were seldom formed individually, but several kink bands were formed close together by deformation in many cases, as shown in Fig. 3. Their formation was not very homogeneous, and deformation kink bands were roughly aggregated at 70–410 μm intervals along the lateral direction in the plate-like grains. Polishing the specimen surface after the first deformation caused the traces of the basal slip and deformation kink boundaries to vanish entirely, as shown in Fig. 5(b). A small specimen was cut from the deformed specimen, then a subsequent deformation at 45° orientation was applied at temperatures ranging from ambient to 400 °C.

Fig. 6(a) shows the deformation microstructure introduced by the second deformation at room temperature. Slip traces parallel to the grain interface, i.e., basal slip traces, were abundantly introduced via the second deformation. In addition, the boundaries of the deformation kink bands again appeared clearly, even though they had vanished after polishing prior to the second deformation, as shown in Fig. 5(b). The introduced basal slip traces were significantly bent in a zigzag manner parallel to the bending interface of the plate-like grain. At ambient temperature, the basal slip traces sometimes propagated beyond a kink boundary, but they often stopped at the boundaries of the deformation kink bands, as shown in Fig. 6(a). Note that at the point where the propagation of the basal slip ended, “secondary deformation kink bands” were sometimes formed inside the initial deformation kink bands, as indicated by small red arrows. This implies that strong stress concentration occurs at the kink band boundary, which indicates that a deformation kink band hinders motion of basal dislocations, as expected. Similar features were also observed after deformation at 100 and 200 °C, as shown in Fig. 6(b) and (c), respectively. However, the stopping frequency of the basal slip at the deformation kink boundary was reduced above 300 °C, and the basal slip often propagated a long distance beyond the kink boundary, as shown in Fig. 6(d) and (e). At 400 °C, in addition to basal slips, the slip traces that were not parallel to the grain interface sometimes appeared near a deformation kink band, as indicated by the double blue arrows in Fig. 6(e). The previous study demonstrated they must be the traces of prismatic slip [34]. These microstructural observation results imply that the effect of the deformation kink as an obstacle may weaken above 300 °C.

Fig. 7 shows the temperature dependence of the yield stress obtained from double deformation tests at 45° orientation. The graph also shows yield stresses of the virgin DS crystals deformed at 0° and 45° orientations [18] for comparison. At room temperature, the yield stress measured by double compression was nearly double that of the virgin crystal deformed at the 45° orientation, demonstrating that the introduced deformation kink bands strongly increase the yield stress as these hinder the motion of basal dislocations. Similar yield stress increases were measured up to 200 °C. However, the amount of increase compared to the virgin crystal was largely reduced at 300 °C, and the yield stress approached the value in the virgin crystals.

4. Discussion

4.1. Significant difference in yield stress between DS and extruded alloys

In the present study, it was found that the microstructure of an LPSO-phase alloy significantly changes its mechanical properties. The origin of extremely high yield stress in the extruded alloy is discussed in this section based on the present results. Fig. 8 shows a comparison of the yield stress values in the DS alloy and the extruded LPSO-phase alloy reported in previous papers [18,23], where the DS alloy was grown at 5 mm/h and the extruded alloy was fabricated from the as-cast ingot with R10 reduction rate. The yield stress of the extruded alloy exhibits much higher values than that of the DS alloy at 0° and 45° orientation. The results presented in Section 3.1 provide an explanation for why an LPSO-phase extruded alloy exhibits an extremely high yield stress at 0° orientation. The extremely high yield stress of ~460 MPa at ambient temperature and 0° orientation was predominantly attributed to the high formation stress of the deformation kink, which was brought about by the refined microstructure (thickness). The grain thickness is ~101 μm in the DS alloy, but it is ~10 μm in the extruded alloy.

On the other hand, when the compression test was conducted at 45° orientation, the yield stress greatly decreased compared to that at 0° orientation in both alloys. This was the result of frequent basal slip, because the Schmid factor for basal slip exhibits high values in many

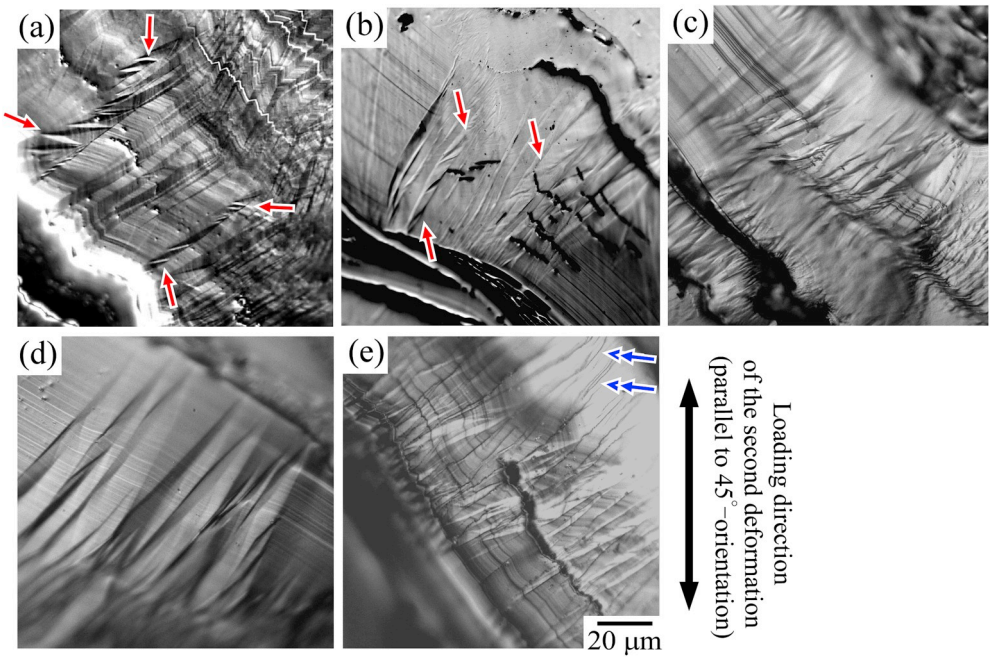

Fig. 6. OM images showing the microstructures of specimens after the double compression tests. The second deformation at 45° orientation was performed at (a) room temperature, (b) 100 °C, (c) 200 °C, (d) 300 °C, and (e) 400 °C.

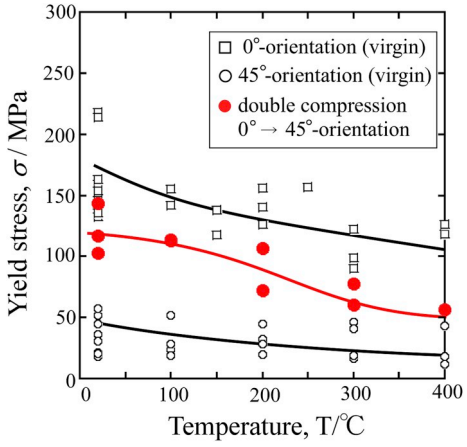

Fig. 7. Temperature dependence of yield stress measured from double compression tests. The yield stresses of the virgin DS crystals deformed at 0° and 45° orientation [18] are also plotted in the graph for comparison.

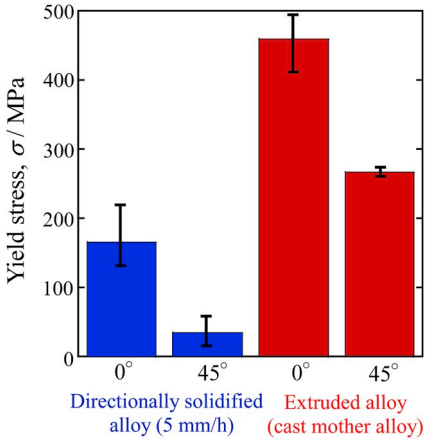

Fig. 8. Comparison of the yield stress values in DS and extruded alloys evaluated from room temperature compression tests at 0° and 45° orientations [18,23].

grains at 45° orientation as a result of the basal fiber texture; this was confirmed in the DS crystal [18]. Indeed, basal slip could be confirmed to occur in the extruded alloy from the deformation microstructure shown in Fig. 9. However, it is noteworthy that although the yield stress of the extruded alloy showed a large reduction compared to that of 0° orientation, the absolute value of the yield stress at 45° orientation was still as high as ~270 MPa. This value was ~8 times higher than that of the DS crystals (~35 MPa). Nevertheless, the basal slip controlled the deformation behavior in both alloys. This must be closely related to the influence of the pre-existing deformation kink bands in the extruded specimens, which were introduced during extrusion, in addition to the initial grain refinement effect. In order to show this quantitatively, the following section discusses mechanism governing deformation and the origin of high yield stress in the extruded alloy at 45° orientation.

4.2. Kink-band strengthening acting in the extruded alloy deformed at 45° orientation

Fig. 10 shows the relationship between the yield stress and the inverse of the square root of the length of the LPSO-phase grains in the annealed LPSO-phase alloys in which basal fiber texture was collapsed. In this graph, the results reported in previous papers [21,22] was further updated, and in addition the yield stresses of the extruded alloy deformed at 45° orientation and at room temperature, 200, and 300 °C reported in Ref. [23] were added as solid symbols. As described in the Introduction, the yield stress of the LPSO-phase alloys with random texture obeyed the so-called Hall-Petch relation $\sigma_y = \sigma_0 + kd^{-1/2}$. The "length" of the long-axis of the plate-like LPSO-phase grains was taken as the grain size d because the mean-free path of the basal dislocation was directly proportional to the average length of the long-axis of the grain size due to the peculiar plate-like shape of the LPSO-phase grains parallel (0001) [21]. As shown in Fig. 9, deformation of the extruded alloy at the 45° orientation is also dominantly carried by basal slip

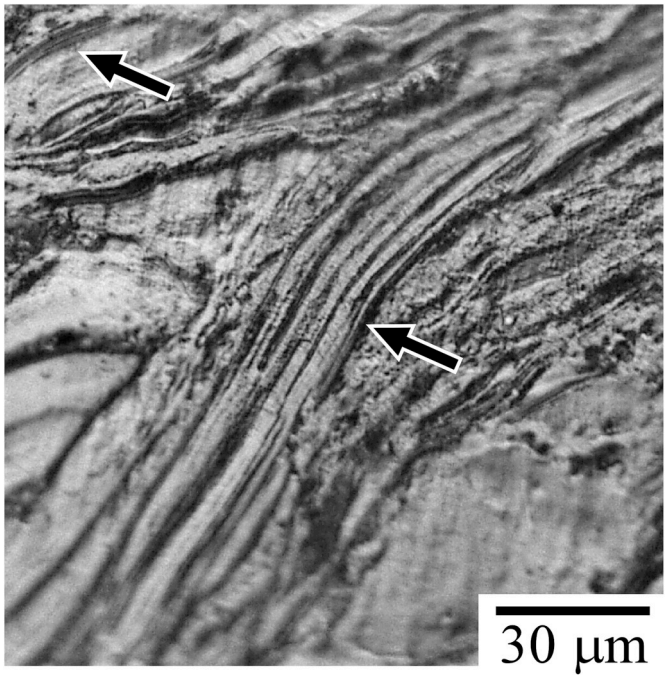

Fig. 9. OM image showing the deformation microstructure of the extruded specimen compressed at 45° orientation at room temperature. Basal slip traces are indicated with small arrows.

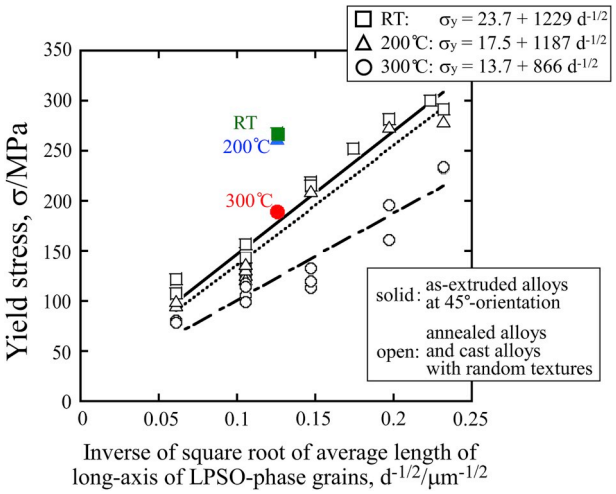

Fig. 10. Comparison of the yield stress values of the as-extruded alloy deformed at 45° orientation [23] and that in annealed and cast LPSO-phase alloys in which basal fiber texture was collapsed [21,22], in which some data was further updated. The yield stress is plotted as a function of inverse of square root of average grain length, i.e., a so-called Hall-Petch plot.

because the Schmid factor for basal slip exhibits high values in many grains at this 45° orientation. Nevertheless, as shown in Fig. 10, the yield stress measured from compression tests exhibited much higher values than predicted with the Hall-Petch relation. The increased yield stress compared to that estimated with the Hall-Petch relation was significant at room temperature and at 200 °C. At 300 °C, the increased yield stress compared to the value anticipated from the Hall-Petch relation was maintained, but the deviation became smaller than those at room temperature and 200 °C. It must be noted that the observed temperature dependence of the stress increment compared with the Hall-Petch relation is similar to the results in Fig. 7; the effect of the kink deformation band as an obstacle to basal slip deformation is effective at and below 200 °C, while the effect is reduced at 300 °C. In the extruded alloy, the apparent average grain length (straight part nearly along the extrusion direction) was ~65 μm, which was somewhat shorter than that in the as-cast alloy of ~90 μm, owing to the bending of the grains by kink-band formation. Here, if the grain length in the extruded alloys is assumed to be further reduced to ~25 μm ($d^{-1/2}$ = ~0.2), the obtained yield stress agrees well with the Hall-Petch estimation. This suggests that the formation of kink deformation bands in the grain strongly affects the mechanical properties of the LPSO-phase alloy by inducing dynamical microstructure refinement, thus strengthening the alloy.

The effect of the deformation kink band boundary as the extra grain boundary could be further confirmed by comparing the features of the stress-strain curves. Fig. 11(a) shows the stress-strain curves for the extruded alloy, double compressed DS crystal, and original DS crystal deformed at 45° orientation and room temperature. Fig. 11(b) shows variations in the work-hardening rate with plastic strain, which were evaluated by calculating the differential value dσ/dε from the stress-strain curves. In the stress-strain curve for the virgin DS crystal, a very long plateau corresponding to the "stage I region" appeared just after yielding, and the work-hardening rate was moderate. In contrast, the stress-strain curve of the extruded alloy indicates strong work hardening, especially during the early stage of deformation, and the flow stress continued to show a gradual increase. These features are similar to those measured in the double-compressed alloy, as shown in Fig. 11(a) and (b). These prove that the deformation kink band boundary strongly hinders deformation in the extruded alloy deformed at 45° orientation.

4.3. Quantitative evaluation of the kink-band strengthening

As a more quantitative evaluation of the influence of the deformation kink band on basal slip, the relation between the yield stress evaluated from double compression tests and the pre-existing aggregated kink band interval in the specimen was analyzed by comparing with the Hall-Petch relationship for basal slip shown in Fig. 10. If the aggregated kink bands provide the same hindrance as the grain boundary, the yield stress from the double compression test should match that determined from the Hall-Petch relationship by assuming the aggregated kink band interval to be the grain size. The analytical deformation results at room temperature and 300 °C are shown in Fig. 12(a) and (b), respectively. As described in section 3.2, the pre-existing deformation kink bands formed inhomogeneously in specimens but aggregated at roughly 70–410 μm intervals during the first deformation step in the double compression tests. The aggregated interval is indicated on the horizontal axis as an "apparent grain length" distribution. Variations (error bar) in the yield stress measured from double compression tests are indicated on the vertical axis, and the region where they cross is indicated with the hatched region. At room temperature, the line showing the Hall-Petch relationship nearly passes the center of the hatched region, which demonstrates that the aggregated deformation kink bands effectively hinder dislocation motion, similar to the grain boundaries. According to Nizolek et al. [36], in the wedge-type kink band in which the kink band boundary is terminated in the matrix, a strong elastic strain field exist at the tip of the kink band. This strain field might enhance the hindrance against dislocation motion as it approaches the kink band boundary. Whether or not such an additional effect exists in the kink band boundary in the LPSO phase could not be precisely evaluated in the present study due to the large scatter in the data. Further studies are required to clarify this.

Furthermore, the line showing the Hall-Petch relationship at 300 °C passed through the hatched region in Fig. 12(b), indicating that the kink boundary acts as an obstacle even at 300 °C. However, the obtained yield stress from double compression tests seems to be somewhat lower than the expected value from the Hall-Petch relation. This suggests that the effect of aggregated deformation kink bands as obstacles may become weaker than that of a random grain boundary at 300 °C.

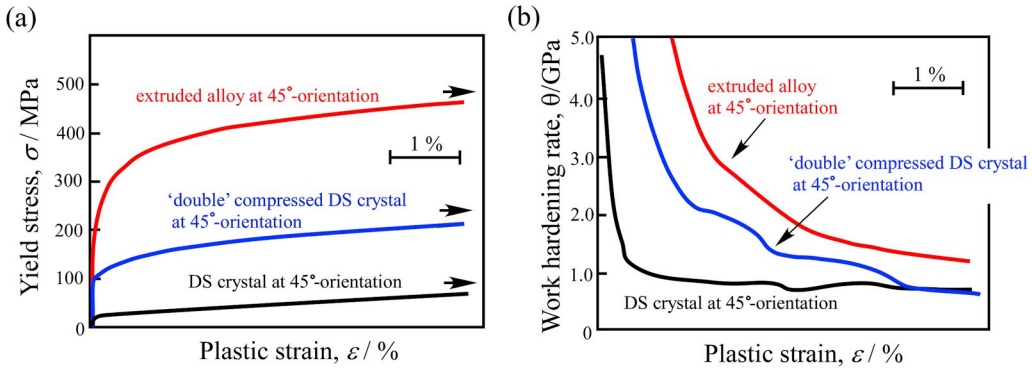

Fig. 11. (a) Stress-strain curves of the extruded alloy, double compressed DS crystal, and virgin DS crystal deformed at 45° orientation at room temperature. (b) Variations in the work-hardening rate with plastic strain.

This was reflected in the deformation microstructure as the basal slip stopping frequency reduced at the deformation kink boundary above 300 °C, as shown in Fig. 6(d) and (e).

In these ways, it was found that the introduction of a deformation kink band is very effective for strengthening the LPSO-phase. This effect is strong at low temperatures but is somewhat weakened above 300 °C. This implies that the mechanism controlling deformation changes at high temperatures. One possibility is that the mechanism controlling basal slip itself may vary at high temperatures, accompanied by frequent cross-slip and/or climbing motion. This is expected from a study using the DS crystal; the strain-rate sensitivity of the flow stress loaded at 45° orientation where basal slip predominately occurs was negligible at room temperature, but it increased at high temperatures (~400 °C) [35]. This indicates that the mechanism controlling dislocation motion changes to one that requires a relatively strong thermally activated process at high temperature. In addition, the increased frequency of non-basal slip, i.e. prismatic slip, at high temperatures is also considered to be another plausible factor. The critical resolved shear stress (CRSS) for prismatic slip has not yet been accurately determined, but it is supposed to show a strong temperature dependence [34]. Non-basal slip was hardly observed from double compression tests at low temperatures, but it sometimes appeared at 400 °C, as shown in Fig. 6(e). This suggests that it would occur locally near the kink deformation band and would accommodate stress concentration caused by the pile-up of basal dislocations, at high temperatures. According to the results in Fig. 12(b), the hindrance provided by the deformation kink boundary might be weakened to a greater extent than the hindrance from a random boundary at high temperatures under these accommodated process related to the non-basal slips. To clarify the further detailed reasons for this, TEM study on the deformation microstructure is now proceeding with the goal of understanding the high temperature deformation mechanisms in LPSO-phase alloys. In addition, more quantitative evaluation on the variations in stopping frequency of slip trace at the kink band boundary, formation frequency of the secondary kink band etc. with deformation temperature and LPSO-phase composition is now in progress to clarify the detailed mechanism of the kink-band strengthening.

In this way, it was found that the LPSO-phase can be strengthened by refining the microstructure and introducing deformation kink bands. To develop an effective strategy for kink-band strengthening, the influence of the volume fraction and misorientation (rotation) angle of kink bands which must be dependent on the applied stress, and the introducing temperature of kink bands (first deformation temperature in Fig. 5(a)) on the strengthening behavior of the LPSO-phase must be further clarified in the future study. As we previously reported, the LPSO-phase acts as an effective and important reinforcement via a short-fiber-like mechanism in Mg/LPSO two-phase extruded alloys [4,9]. Therefore, strengthening the LPSO-phase through these processes directly contributes to enhancing the mechanical properties of these two-phase alloys. For the further development of the Mg/LPSO two-phase alloy with superior mechanical properties, the variations in mechanical properties with alloy composition; i.e. volume fraction of the LPSO-phase, must be more precisely clarified, including the variation in formation behavior of the kink band in them.

5. Conclusions

In this study, the microstructural factors that govern the strength of the LPSO-phase were examined using the alloys in which the microstructures were significantly varied via directional solidification and

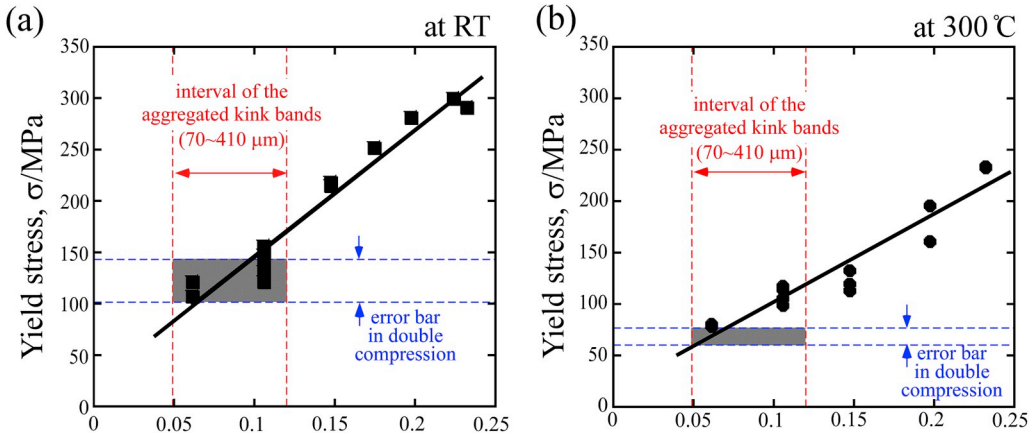

Fig. 12. Relation between the pre-existing kink band aggregate interval and yield stress from double compression tests at (a) room temperature and (b) 300 °C. These are displayed in a Hall-Petch plot of basal slip in annealed and cast LPSO-phase alloys in which basal fiber texture was collapsed [21,22].

extrusion processes. The obtained results are summarized as follows:

(1) The experimental results clarified that the microstructure refinement significantly contributes to strengthening the LPSO-phase alloy via two different mechanisms. In addition to the effect of reduction in the length of the plate-like LPSO-phase grains on the basal slip reported in the previous study, it was newly suggested that the formation stress of the deformation kink band can be increased by reducing the thickness of the plate-like LPSO-phase grains. This significantly contributes to strengthening the alloy with basal fiber texture, i.e. the extruded alloys.
(2) The deformation kink bands effectively hinder the motion of basal dislocations. Therefore, the introduced deformation kink bands largely contributed to strengthening the alloy against further deformation via a Hall-Petch-like mechanism. The increased yield stress due to the introduced kink bands is significant at and below 200 °C, but the effect gradually becomes weak above 300 °C accompanied by activation of non-basal slip. This kink-band strengthening is one predominant reason why the LPSO-phase extruded alloy exhibits an unusually high yield stress at any loading orientation.

Declarations of interest

None.

Author contributions

K. Hagihara designed the study and wrote the manuscript. K. Hagihara and M. Yamasaki carried out the experiments. Then, the results were discussed by all authors. All authors approved the final article.

Acknowledgement

This work was supported by Japan Society for the Promotion of Science (JSPS) KAKENHI for Scientific Research on Innovative Areas “MFS Materials Science” (Grant Numbers: JP18H05478, JP18H05476 and JP18H05475), and also partly supported by JSPS KAKENHI JP18H05254.

References

[1] M.K. Kulekci, Magnesium and its alloys applications in automotive industry, Int. J. Adv. Manuf. Technol. 39 (2008) 851–865.
[2] Y. Kawamura, K. Hayashi, A. Inoue, T. Masumoto, Rapidly solidified powder metallurgy $Mg_{97}Zn_1Y_2$ alloys with excellent tensile yield strength above 600 MPa, Mater. Trans. 42 (2001) 1172–1176.
[3] M. Yamasaki, T. Anan, S. Yoshimoto, Y. Kawamura, Mechanical properties of warm-extruded Mg–Zn–Gd alloy with coherent 14H long periodic stacking ordered structure precipitate, Scr. Mater. 53 (2005) 799–803.
[4] K. Hagihara, A. Kinoshita, Y. Sugino, M. Yamasaki, Y. Kawamura, H.Y. Yasuda, Y. Umakoshi, Effect of long-period stacking ordered phase on mechanical properties of Mg97Zn1Y2 extruded alloy, Acta Mater. 58 (2010) 6282–6293.
[5] X.H. Shao, Z.Q. Yang, X.L. Ma, Strengthening and toughening mechanisms in Mg–Zn–Y alloy with a long period stacking ordered structure, Acta Mater. 58 (2010) 4760–4771.
[6] M. Yamasaki, K. Hashimoto, K. Hagihara, Y. Kawamura, Effect of multimodal microstructure evolution on mechanical properties of Mg–Zn–Y extruded alloy, Acta Mater. 59 (2011) 3646–3658.
[7] E. Oñorbe, G. Garcés, P. Pérez, P. Adeva, Effect of the LPSO volume fraction on the microstructure and mechanical properties of Mg–Y_{2X}–Zn_X alloys, J. Mater. Sci. 47 (2012) 1085–1093.
[8] J. Wang, P. Song, X. Zhou, X. Huang, F. Pan, Influence of the morphology of long-period stacking ordered phase on the mechanical properties of as-extruded Mg–5Zn–5Y–0.6Zr magnesium alloy, Mater. Sci. Eng. A 556 (2012) 68–75.
[9] K. Hagihara, A. Kinoshita, Y. Fukusumi, M. Yamasaki, Y. Kawamura, High-temperature compressive deformation behavior of Mg97Zn1Y2 extruded alloy containing a long-period stacking ordered (LPSO) phase, Mater. Sci. Eng. A 560 (2013) 71–79.
[10] E. Oñorbe, G. Garcés, F. Dobes, P. Pérez, P. Adeva, High-temperature mechanical behavior of extruded Mg-Y-Zn alloy containing LPSO phases, Metall. Mater. Trans. A 44 (2013) 2869–2883.
[11] L.B. Tong, X.H. Li, H.J. Zhang, Effect of long period stacking ordered phase on the microstructure, texture and mechanical properties of extruded Mg–Y–Zn alloy, Mater. Sci. Eng. A 563 (2013) 177–183.
[12] G. Garces, P. Perez, S. Cabeza, H.K. Lin, S. Kim, W. Gan, P. Adeva, Reverse tension/compression asymmetry of a Mg-Y-Zn alloys containing LPSO phases, Mater. Sci. Eng. A 647 (2015) 287–293.
[13] J.K. Kim, S. Sandlöbes, D. Raabe, On the room temperature deformation mechanisms of a Mg-Y-Zn alloy with long-period-stacking-ordered structures, Acta Mater. 82 (2015) 414–423.
[14] H. Liu, J. Bai, K. Yan, J. Yan, A. Ma, J. Jiang, Comparative studies on evolution behaviors of 14H LPSO precipitates in as-cast and as-extruded Mg-Y-Zn alloys during annealing at 773 K, Mater. Des. 93 (2016) 9–18.
[15] R. Chen, S. Sandlöbes, X. Zeng, D. Li, S. Korte-Kerzel, D. Raabe, Room temperature deformation of LPSO structures by non-basal slip, Mater. Sci. Eng. A 682 (2017) 354–358.
[16] G. Garcés, K. Máthis, J. Medina, K. Horváth, D. Drozdenko, E. Oñorbe, P. Dobroň, P. Pérez, M. Klaus, P. Adeva, Combination of in-situ diffraction experiments and acoustic emission testing to understand the compression behavior of Mg-Y-Zn alloys containing LPSO phase under different loading conditions, Int. J. Plast. 106 (2018) 107–128.
[17] E. Abe, A. Ono, T. Itoi, M. Yamasaki, Y. Kawamura, Polytypes of long-period stacking structures synchronized with chemical order in a dilute Mg–Zn–Y alloy, Philos. Mag. Lett. 91 (2011) 690–696.
[18] K. Hagihara, N. Yokotani, Y. Umakoshi, Plastic deformation behavior of $Mg_{12}YZn$ with 18R long-period stacking ordered structure, Intermetallics 18 (2010) 267–276.
[19] K. Hagihara, Y. Sugino, Y. Fukusumi, Y. Umakoshi, T. Nakano, Plastic deformation behavior of $Mg_{12}ZnY$ LPSO-phase with 14H-typed structure, Mater. Trans. 52 (2011) 1096–1103.
[20] K. Hagihara, T. Okamoto, H. Izuno, M. Yamasaki, M. Matsushita, T. Nakano, Y. Kawamura, Plastic deformation behavior of 10H-type synchronized LPSO phase in a Mg-Zn-Y system, Acta Mater. 109 (2016) 90–102.
[21] K. Hagihara, A. Kinoshita, Y. Sugino, M. Yamasaki, Y. Kawamura, H.Y. Yasuda, Y. Umakoshi, Plastic deformation behavior of Mg89Zn4Y7 extruded alloy composed of long-period stacking ordered phase, Intermetallics 18 (2010) 1079–1085.
[22] K. Hagihara, A. Kinoshita, Y. Sugino, M. Yamasaki, Y. Kawamura, H.Y. Yasuda, Y. Umakoshi, Temperature dependence of compressive deformation behavior of Mg89Zn4Y7 extruded LPSO-phase alloys, Mater. Sci. Forum 638–642 (2010) 607–610.
[23] K. Hagihara, Z. Li, M. Yamasaki, Y. Kawamura, T. Nakano, Strengthening mechanisms acting in extruded Mg-based long-period stacking ordered (LPSO)-phase alloys, Acta Mater. 15 (2019) 226–239.
[24] J.B. Hess, C.S. Barrett, Structure and nature of kink bands in zinc, Trans. Am. Inst. Min. Met. Eng. 185 (1949) 599–606.
[25] M.W. Barsoum, T. El-Raghy, Room temperature ductile carbides, Metall. Mater. Trans. A 30A (1999) 363–369.
[26] M.W. Barsoum, T. Zhen, A. Zhou, S. Basu, S.R. Kalidindi, Microscale modeling of kinking nonlinear elastic solids, Phys. Rev. B 71 (2005) 134101.
[27] T. Zhen, M.W. Barsoum, S.R. Kalidindi, Effects of temperature, strain rate and grain size on the compressive properties of Ti_3SiC_2, Acta Mater. 53 (2005) 4163–4171.
[28] A.G. Zhou, M.W. Barsoum, Kinking nonlinear elastic deformation of Ti_3AlC_2, Ti_2AlC, $Ti_3Al(C_{0.5},N_{0.5})_2$ and $Ti_2Al(C_{0.5},N_{0.5})$, J. Alloy. Comp. 498 (2010) 62–70.
[29] F.C. Frank FC, A.N. Stroh, On the theory of kinking, Proc. Phys. Soc. Sect. B 65 (1952) 811–821.
[30] K. Hagihara, A. Kinoshita, Y. Fukusumi, M. Yamasaki, Y. Kawamura, Microstructural factors affecting the deformation behavior of $Mg_{12}ZnY$ LPSO-phase alloys, Mater. Sci. Forum 706–709 (2012) 1158–1163.
[31] X.H. Shao, Z.Z. Peng, Q.Q. Jin, X.L. Ma, Atomic-scale segregations at the deformation-induced symmetrical boundary in an Mg-Zn-Y alloy, Acta Mater. 118 (2016) 177–186.
[32] Z.Z. Peng, X.H. Shao, Q.Q. Jin, J.F. Liu, X.L. Ma, Dislocation configuration and solute redistribution of low angle kink boundaries in an extruded Mg–Zn–Y–Zr alloy, Mater. Sci. Eng. A 687 (2017) 211–220.
[33] T. Matsumoto, M. Yamasaki, K. Hagihara, Y. Kawamura, Configuration of dislocations in low-angle kink boundaries formed in a single crystalline long-period stacking ordered Mg-Zn-Y alloy, Acta Mater. 151 (2018) 172-124.
[34] K. Hagihara, Y. Fukusumi, M. Yamasaki, T. Nakano, Y. Kawamura, Non-basal slip systems operative in $Mg_{12}ZnY$ long-period stacking ordered (LPSO) phase with 18R and 14H structures, Mater. Trans. 54 (2013) 693–697.
[35] K. Hagihara, Z. Li, M. Yamasaki, Y. Kawamura, T. Nakano, Strain-rate dependence of deformation behavior of LPSO-phases, Mater. Lett. 214 (2018) 119–122.
[36] T.J. Nizolek, M.R. Begley, R.J. McCabe, J.T. Avallone, N.A. Mara, I.J. Beyerlein, T.M. Pollock, Strain fields induced by kink band propagation in Cu-Nb nanolaminate composites, Acta Mater. 133 (2017) 303–315.